0021-972X/04/$15.00/0
Printed in U.S.A.

The Journal of Clinical Endocrinology & Metabolism 89(10):5222–5232

doi: 10.1210/jc.2004-0331

Specificity and Regioselectivity of the Conjugation of Estradiol, Estrone, and Their Catecholestrogen and Methoxyestrogen Metabolites by Human Uridine Diphospho-glucuronosyltransferases Expressed in Endometrium

JOHANIE LÉPINE, OLIVIER BERNARD, MARIE PLANTE, BERNARD TÊTU, GEORGES PELLETIER, FERNAND LABRIE, ALAIN BÉLANGER, AND CHANTAL GUILLEMETTE

Canada Research Chair in Pharmacogenomics (C.G.); Centre de Recherche du Centre Hospitalier de l'Université Laval, Department of Molecular Endocrinology and Oncology (J.L., O.B., G.P., F.L., A.B., C.G.), G1V 4G2 Québec, Canada; Laval University, Faculty of Pharmacy (J.L., O.B., C.G.), Faculty of Medicine, Gynecologic Oncology Service, Hôtel-Dieu de Québec (M.P.), Department of Pathology Hôtel-Dieu de Québec (B.T.), G1K 7P4 Québec, Canada

Uridine diphospho-glucuronosyltransferases (UGTs) inactivate and facilitate the excretion of estrogens to glucuronides (-G), the most abundant circulating estrogen conjugates. The identity of the conjugated estrogens formed by all known overexpressed UGTs (n = 16) was analyzed by comparison with retention time and mass fragmentation of authentic standards by HPLC tandem mass spectrometry methods. Six UGTs, namely 1A1, 1A3, 1A8, 1A9, 1A10, and 2B7, were found to glucuronidate estradiol (E_2) and estrone (E_1), their hydroxyls (OH), and their methoxy derivatives (MeO). Addition of glucuronic acid was catalyzed by specific UGTs at positions 2, 3, and 4 of the estrogens, whereas only E_2 was conjugated at position 17 by UGT2B7. Kinetic parameters indicate that the conjugation of E_2 at position 3 was predominantly catalyzed by 1A1, 1A3, and 1A8 and by 1A8 for E_1. Conjugation of 2-OHE_1/E_2 and 2- and 4-$MeOE_1$/E_2 was selective at position 3, mostly catalyzed by 1A1 and 1A8. Of all UGTs, UGT2B7 demonstrated the highest catalytic activities for estrogens and at least 10- to 50-fold higher activity for the conjugation of genotoxic 4-hydroxycatecholestrogens at position 4, compared with the conjugation of E_2, E_1, and 2-hydroxycatecholestrogens. Its presence was further shown in the endometrium by RT-PCR and immunohistochemistry, localizing in the same cells expressing CYP1B1, involved locally in the formation of 4-hydroxycatecholestrogens. Data show that several UGT enzymes detected in the endometrium are involved in the glucuronidation of E_2 and its 2-OH, 4-OH, and 2-MeO metabolites that exert various biological effects in the tissue. (*J Clin Endocrinol Metab* 89: 5222–5232, 2004)

EXPOSURE OF ESTROGEN-SENSITIVE tissues to excessive stimulation by natural or synthetic estrogens is considered as a significant factor in the induction and the development of cancers (1, 2). As a key determinant in estrogen action, the intracellular concentration of estrogens is dependent not only on circulating estrogen levels but also on *in situ* or intracrine formation and local metabolism in estrogen-sensitive tissues (3, 4). A number of studies have clearly demonstrated that estrogen target tissues are the site of modification of estrogen action through conversion of estrogens into the hydroxylated derivatives catechol estrogens (CEs) by cytochromes P450 (CYP), which mainly oxidize estrogen into 2-hydroxy-CE [2-OH-estrone (E_1)/estradiol (E_2)] and 4-hydroxy-CE (4-OHE_1/E_2), and the catechol-*O*-methyltransferase (COMT) that converts CEs to methyl-CE (MeOCEs) (5, 6).

Recent findings highlight the importance of CE metabolites as chemical mediators and their link to cancer development and progression (7–9). For instance, 4-OHE_2 undergoes metabolic redox cycling to generate reactive oxygen species, which may damage lipids and DNA and initiate estrogen-related carcinogenesis (10). By contrast, biotransformation of CE to 2-MeOCE may result in the formation of a protective metabolite having very potent inhibitory effect on cell proliferation, tubulin activity, and angiogenesis (11–13). The formation of CEs and MeOCEs may proceed through reactions carried out by hepatic metabolism but also through local metabolic conversion in extrahepatic hormone responsive organs or through a combination of both. Because of their unique chemical and biological properties, it is critical to establish the contribution of extrahepatic formation and elimination of estrogen and of their metabolites.

Conjugation transforms estrogenic hormones into less active, more polar and water-soluble metabolites, thus facilitating their excretion in the bile and urine. Conjugative estrogen metabolism includes sulfonation (14) and glucu-

Abbreviations: CE, Catecholestrogen; COMT, catechol-*O*-methyltransferase; CYP, cytochrome P450; E_1, estrone; E_2, estradiol; -G, glucuronide; GAPDH, glyceraldehyde-3-phosphate dehydrogenase; HEK, human embryonic kidney; K_m, substrate concentration at half-maximal velocity; 2-MeOCE, 2-methoxycatecholestrogen; 4-MeOCE, 4-methoxycatecholestrogen; MRM, multiple reaction monitoring; MS, mass spectrometry; MS/MS, tandem mass spectrometry; 2-OHCE, 2-hydroxycatecholestrogen; 4-OHCE, 4-hydroxycatecholestrogen; UGT, uridine diphospho-glucuronosyltransferase; V_{max}, maximal velocity.

JCEM is published monthly by The Endocrine Society (http://www.endo-society.org), the foremost professional society serving the endocrine community.

ronidation (15–18), two reactions catalyzed by sulfotransferases and uridine diphospho-glucuronosyltransferases (UGTs), respectively. In fact, sulfates and glucuronides are the most abundant circulating estrogen conjugates (19), whereas estrogen sulfates represent a form of estrogen storage that acts as a precursor of E_2 (14). On the other hand, glucuronidation by UGTs leads to complete inactivation of estrogen (17, 19). To the best of our knowledge, human β-glucuronidase activity has never been reported in the literature for the endometrium. Glucuronidation of steroids is not limited to the liver, and this metabolic pathway is recognized as contributing significantly to the modulation of specific physiological effects of steroids in target tissues such as the prostate (15, 20–22). Furthermore, the detection of significant amounts of estrogen glucuronides in the breast cystic fluid supports the role of the glucuronidation metabolism in the elimination of estrogens (23, 24). The presence of UGTs was reported in several estrogen target organs such as the breast and uterus (15, 25, 26), even though a comprehensive analysis of the expression of every UGT enzyme reactive toward estrogens in target tissues has never been completed. Several human UGTs are known to exert catalytic activities toward E_2, E_1, and their hydroxylated metabolites, whereas the glucuronidation of MeOCE remains to be clarified (17, 18, 27–30). To date, 16 functional UGT proteins have been reported (31, 32). *In vitro* studies using human UGT cDNAs cloned and expressed in mammalian cells have been used to determine the specificity of UGT isoenzymes for some estrogens in a small number of studies (15, 17, 18, 28–30), whereas a systematic study using the same experimental conditions remains to be conducted. The detailed regioselectivity of UGTs has never been systematically established, possibly because of the lack of estrogen glucuronide standards and suitable analytical methods.

In the present study, we hypothesized that E_2, E_1, and their oxidatized metabolites undergo glucuronidation at various positions and that these site-specific reactions are catalyzed by different UGTs. Given that the enzymatic machinery for the formation of catechol and methoxy metabolites of estrogen was demonstrated in the uterus (5, 6), it was expected that UGT involved in the glucuronidation of estrogen would also be expressed. We have first developed a highly sensitive and specific mass spectrometry-based analytical method to thoroughly establish the substrate specificity and stereoselectivity of all known functional human UGT proteins toward E_2 and E_1 and their hydroxyl as well as their MeOCE derivatives under the same experimental conditions. In the course of this study, we accumulated data on the enzymatic kinetics [maximal velocity (V_{max}), substrate concentration at half-maximal velocity (K_m), and catalytic efficiencies] of individual UGT isoforms to determine which UGTs are the most efficient in catalyzing glucuronidation at the 2-, 3-, 4-, and 17-hydroxyl positions of estrogens and define their stereoselectivity. Subsequently we explored the expression of UGT2B7 that metabolizes with the highest catalytic efficiency the genotoxic 4-OHCEs in the uterus by RT-PCR and immunohistochemistry using a specific antibody. Altogether, the data indicate that glucuronidation of estrogen may be one of the mechanisms of major biological significance in the inactivation and elimination of estrogens, their reactive CEs, and MeOCE metabolites in the uterus.

Materials and Methods

Chemicals

E_1, E_2, 2-OHE_1, 4-OHE_1, 2-OHE_2, 4-OHE_2, 2-$MeOE_1$, 4-$MeOE_1$, 2-$MeOE_2$, 4-$MeOE_2$, E_1-3G, E_2-3G, and E_2-17G were purchased from Steraloids (Newport, RI). The glucuronide derivatives of 2-OHE_1, 4-OHE_1, 2-OHE_2, 4-OHE_2, 2-$MeOE_1$, 4-$MeOE_1$, 2-$MeOE_2$, and 4-$MeOE_2$ were synthesized by Endorecherche (Québec, Canada), and confirmation of the structure of each product was determined by nuclear magnetic resonance. Methanol (HPLC grade), acetonitrile (HPLC grade), 1-chlorobutane (HPLC grade), and iso-amyl-alcohol were obtained from VWR Canlab (Montréal, Canada). Ammonium hydroxide (trace metal grade) was purchased from Fisher Scientific (Nepean, Canada).

Characterization of human embryonic kidney (HEK)293 cell systems expressing UGT1A and UGT2B

Microsomal proteins used for UGT expression were prepared as previously described (33–35). To ascertain the level of UGT protein expression in the stable UGT1A- and UGT2B-HEK293 clones, a semiquantitative immunoblot analysis method was used. The microsomal fractions from UGT-HEK293 cells were used in all enzymatic assays, whereas in the case of UGT1A10, commercial microsomal fractions of Sf-9 insect cells infected with a baculovirus strain containing human UGT1A10 cDNA were used (Panvera, Madison, WI). Microsomal proteins (10 μg protein) were separated on SDS-PAGE and transferred onto nitrocellulose. For quantification of the UGT1A proteins, we used the antihuman UGT1A common carboxyl terminus region (amino acids 312–531) antiserum RC-71, as previously reported (15, 34, 35). UGT2B protein levels were quantified using the antihuman UGT2B antibody (EL-93), as previously described (36). To normalize sample loading, blots were stripped and reprobed with anticalnexin antibody (Stressgen Biotechnologies, Victoria, Canada) to detect a second endoplasmic reticulum-resident protein, calnexin. Bands were visualized using enhanced chemiluminescence (Amersham, Piscataway, NJ) and quantified by Bioimage Visage 110s from Genomic Solutions Inc. (Ann Arbor, MI). Ratios between UGT and calnexin signals were calculated for each UGT except for UGT1A10 baculosome for which the UGT signal alone was considered for the expression level.

Assay of UGT activity

Microsomal fractions from UGT-HEK293 cells and commercial microsomal fraction of UGT1A10 were used in enzymatic assays. Reactions (100 μl volume) contained 50 mM Tris-HCl (pH.7.5), 10 mM $MgCl_2$, 100 μg/ml phosphatidylcholine, 8.5 mM saccharolactone, 2 mM uridine diphospho-glucuronic acid, and 40–60 μg membrane protein and steroid substrate (25 μM). Reactions were initiated by adding varying concentrations of each individual substrate. Blanks and controls contained all compounds except steroid substrates and microsomal preparation, respectively. The assays were terminated by adding 100 μl methanol and were centrifuged at 14,000 × *g* for 10 min before analysis. Time-course experiments were designed to determine the linearity of the glucuronidation reaction. All reaction rates were shown to be linear under the selected time interval, and inclusion of detergent was found to be unnecessary for assessment of the full glucuronidating potential of UGT-expressing HEK cell membranes. For determination of V_{max} and K_m values, HEK293 cells stably expressing UGT enzymes were incubated in the presence of varying substrate concentrations from 0.5 to 200 μM for 1 h. Absolute glucuronidation activities were divided by the level of UGT protein and expressed as relative glucuronidation activities in picomoles per minute per milligram.

Mass spectrometry analysis

Incubation medium was diluted with 0.1 ml methanol/water (50:50; vol/vol), vortexed, and then transferred into a conical vial for injection into the mass spectrometer. The HPLC and tandem mass spectrometry (MS/MS) system consisted of a mass spectrometer (model API 3000,

Perkin-Elmer Sciex, Thornhill, Canada) equipped with an elecrospray ionization source in the negative ion mode and a HPLC pump plus autosampler (model 2690, Waters, Milford, MA). A chromatographic separation was achieved with a 100 × 3.9 mm Xterra MS C_8 column 3.5 μm packing material (Waters), using a three-solvent isocratic system (A: water + 0.1% ammonium hydroxide; B: methanol + 0.1% ammonium hydroxide; C: acetonitrile + 0.1% ammonium hydroxide) at a constant flow rate (0.8 ml/min) for 8 min with 90% A, 8.5% B, and 1.5% C. Afterward, the column was washed with 93.5% B and then reequilibrated to initial conditions over 4 min. The mass spectrometer was operated in the multiple reaction monitoring (MRM) mode, and the quantification of the products formed was performed using a calibration curve in the range of 200–10,000 pg/ml of incubation medium for each substrate.

Tissue procurement, RNA purification, reverse transcription, and expression analyses

Nonmalignant uterine tissue was obtained from postmenopausal women who had not received hormone replacement therapy for at least 3 wk and who had no menstrual bleeding for at least 1 yr. All subjects provided written consent for use of their specimens, and the present study was reviewed and approved by Institutional Review Boards (Hôtel-Dieu de Québec, Centre Hospitalier de l'Université Laval Research Center, and Laval University). Fresh material from patients were all collected by the pathologist and immediately deposited in liquid nitrogen within 30 min of surgery pending transfer to a freezer at −80 C. RNA was isolated by the acid guanidium thiocyanate/chloroform method (37). Total RNA was collected with Trizol (Molecular Research Center, Cincinnati, OH), and random hexamers (pDN6) were used to synthesize cDNA from total RNA (1 μg) using a SuperScript II cDNA synthesis kit (Invitrogen, Carlsbad, CA) according to the manufacturer's specifications. Semiquantitative RT-PCR was used to study the expression of the UGT2B7 gene using primers 882 forward: 5′-ctacgtacctgttgttatgtcagaattaac and 883 reverse: 5′-actgatcccacttcttcatgtcaa. For amplification of glyceraldehyde-3-phosphate dehydrogenase (GAPDH), these primers were used: 41 forward: 5′-tgggtgtgaaccatgag and 42 reverse: 5′-cccagcgtcaaaggtgg. PCR products were sequenced. All PCR amplifications were performed using Taq DNA polymerase at 95 C, 30 sec for denaturation, 59 C, 40 sec for annealing, and 72 C, 45 sec for extension in a thermal cycler, with a fixed number of 35 cycles for each pair of primers. GAPDH was used as internal standard.

Characterization of the polyclonal anti-UGT2B7 antibody

Anti-UGT2B7 antibody was raised against amino acids 55–164 (110 amino acids length) of the protein. This fragment corresponds to the portion of the UGT2B7 protein that is the least homologous to other human UGT2B. Several rabbits were injected with a total of 100 μg purified fusion proteins in the presence of incomplete Freund's adjuvant. The production of antibodies was determined 12 d after the injections. To gain information concerning the novel anti-UGT2B7 antibody, Western blot experiments using the recombinant UGT2B7 protein fragment and microsomal proteins from UGT2B7-HK293 cells showed that the immune serum 1809 is immunoreactive for UGT2B7. The specificity of the anti-UGT2B7 1809 antibody was studied by Western blot experiments using microsomal proteins (10 μg) of HK293 cells stably expressing all known UGT2B subfamily members, namely UGT2B4, 2B7, 2B10, 2B11, 2B15, 2B17, and 2B28. Microsomal proteins of human liver were used as positive control. The gel was transferred onto nitrocellulose membrane and incubated with anti-UGT2B7 1809 antibody (dilution 1:2000). Bands were visualized using enhanced chemiluminescence (Amersham) and quantified by Bioimage Visage 110s (Genomic Solutions).

Immunohistochemistry

Six nonmalignant human uterine tissues were also fixed in formol and embedded in paraffin for immunohistochemical studies. The tissues were serially cut at 5-μm and sections mounted on glass slides. The sections were deparaffinized, hydrated, and incubated overnight at 4 C with the human UGT2B7 antiserum diluted 1:250 in Tris-saline (pH 7.6). The sections were then washed and incubated at room temperature for 4 h with peroxidase-conjugated goat antirabbit immunoglobulins (DakoCytomation, Glostrup, Denmark) diluted 1:200 as previously described (38). Endogenous peroxidase activity was eliminated by preincubation with 3% H_2O_2 for 30 min, and peroxidase was then revealed during incubation with 15 mg of 3,3′-diaminobenzidine in 100 ml Tris-saline buffer containing 0.03% H_2O_2. The intensity of the staining was controlled under the microscope. The sections were then counterstained with hematoxylin. Control experiments were performed on adjacent sections by substituting preimmune rabbit serum (1:250).

Enzyme kinetic analysis

Visual inspection of fitted functions [velocity as a function of substrate concentration] and Eadie-Hofstee plots [velocity as a function of (velocity/substrate concentration)] was used to select the best fit enzyme kinetic model (39). These include the Michaelis-Menten model [$V = (V_{max} \times S)/(K_m + S)$], the substrate activation model [Hill equation, $V = (V_{max} \times S^n)/(K_m{}^n + S^n)$] and the uncompetitive substrate inhibition model [$V = (V_{max} \times S)/(K_m + S \times (1 + S/K_s))$], where n is the Hill coefficient or the degree of curve sigmoidicity, and K_s is an inhibition constant. Analysis of data showing sigmoid kinetic was performed using SigmaPlot 8.0 with Enzyme Kinetics 1.1 (SPSS, Chicago, IL), and analysis of data showing substrate inhibition or Michaelis-Menten kinetics was performed using Enzfitter (Biosoft, Ferguson, MO). For Michaelis-Menten and substrate inhibition models, the intrinsic clearance (CL_{int}) estimation values were calculated based on the following equation: $CL_{int} = V_{max}/K_m$, whereas for sigmoid model the maximal clearance (CL_{max}) estimation values were calculated using the following equation: $CL_{max} = (V_{max}/K_m) \times [(n - 1)/(n \times (n - 1)^{1/n})]$ (40).

Results

Analysis of the glucuronidated estrogens by MS

The identity of all conjugated products formed by expressed UGTs was confirmed by comparison with the retention time of HPLC and mass fragmentation of authentic standards using HPLC and tandem MS (MS/MS) methods developed to specifically detect and quantify the E glucuronides. The analyses of those compounds by MS/MS were assessed by MRM mode (parent and daughter ion) to provide higher specificity than single ion monitoring (Table 1). The high accuracy of this analytical method is also achieved by the quality of the chromatographic separation achieved between the two glucuronide products potentially formed from

TABLE 1. Multiple reactions monitoring used in LC/MS/MS detection of estrogens

Steroids	Selected ions (m/z)	
	Parent	Daughter
E_1-3G	445	113
E_1-3G-d_4	449	113
E_2-3G	447	175
E_2-3G-d_4	451	175
E_2-17G	447	74
E_2-17G-d_4	451	74
2-OHE_1-2G	461	285
2-OHE_1-3G	461	285
4-OHE_1-4G	461	285
4-OHE_1-3G	461	285
2-OHE_2-2G	463	287
2-OHE_2-3G	463	287
4-OHE_2-4G	463	287
4-OHE_2-3G	463	287
2-$MeOE_1$-3G	475	113
4-$MeOE_1$-3G	475	113
2-$MeOE_2$-3G	477	113
4-$MeOE_2$-3G	477	113

d_4, Deuterated.

each individual 2-OHCEs and 4-OHCEs. As illustrated in Fig. 1A, despite the same parent and daughter ions for 2-OHE_2-2G and 2-OHE_2-3G, it was possible to chromatographically separate the two estrogen glucuronides. Good chromatographic resolution was also obtained for 4-OHE_2-4G and 4-OHE_2-3G, which also have the same ions (Fig. 1B).

Enzymatic specificity of human UGT enzymes for estrogens

Assays of human UGTs toward a series of estrogens, namely E_1, E_2, 2-OHE_1/E_2, 4-OHE_1/E_2, and their methoxy derivatives 2-$MeOE_1$/E_2 and 4-$MeOE_1$/E_2, were performed using microsomal preparations of HK293 cells engineered to stably express all known human UGTs, with the exception of UGT1A10, which was overexpressed in baculosomes.

The initial screening of the conjugating activity was performed by incubation with the selected microsomal preparation for 16 h containing 25 μM of the estrogenic substrate and 1 mM of glucuronic acid. Most of the UGT2B isoenzymes did not catalyze the glucuronidation of estrogens, except UGT2B7, whereas UGT2B4's activity was minimal (Table 2). On the other hand, several UGT1As were capable of conjugating estrogens with high efficiency, namely UGT1A1, UGT1A3, UGT1A8, UGT1A9, and UGT1A10 (Table 2). The formation of glucuronidated products at positions 2, 3, and 4 of hydroxylated E_2/E_1 was achieved by several UGT isoforms, whereas conjugation at position 17 of 2- and 4-hydroxylated E_2 could not be detected (data not shown).

UGTs with a significant reactivity for at least one of the estrogenic substrates were assayed in further details to determine kinetic parameters (apparent K_m, relative V_{max}, and catalytic efficiencies) (Table 3). The values of apparent K_m and relative V_{max} presented are from one experiment performed in duplicate. Kinetics were repeated for most of the substrates and similar results were obtained in independent experiments. On visual inspection of fitted functions and Eadie-Hofstee plots to select the best fit enzyme kinetic model (39) among Michaelis-Menten, substrate activation, and uncompetitive substrate inhibition, kinetic parameters were calculated using equations described in *Materials and Methods*. The detailed experimentation has allowed us to delineate kinetic properties of UGTs toward estrogens. Various enzymatic kinetic profiles were observed depending on the substrate, especially for E_1, E_2, and 2-OHCEs, and also depending on the products formed as well as the position to which the glucuronic acid is transferred. Similar reports of atypical kinetic properties of human UGTs have recently been published (41, 42).

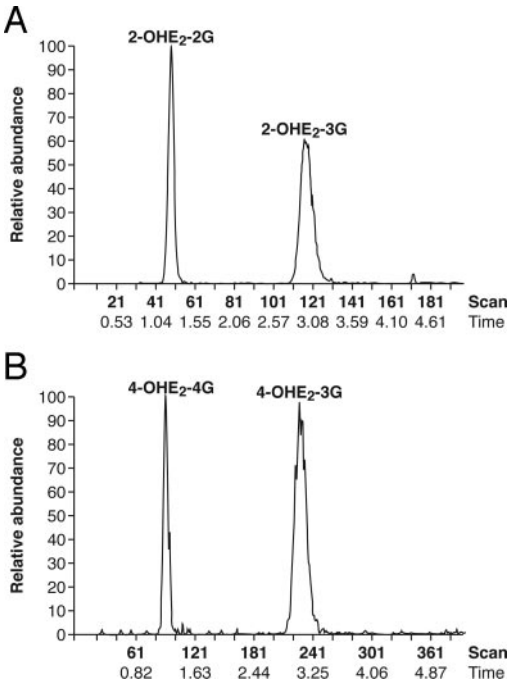

FIG. 1. Chromatographic resolution of the two glucuronide products at position 2, 3, or 4 hydroxyls formed from 2-OHCEs (A) and 4-OHCEs (B). The MS was operated in the MRM mode with mass of 463 and 287 for 2-OHE_2-2G and 2-OHE_2-3G and monitoring of mass 463 and 287 for 4-OHE_2-4G and 4-OHE_2-3G. The chromatographic separation was achieved with a 100 × 3.9-mm Xterra MS C_8 column 3.5-μm packing material, using a three-solvent isocratic system as described in *Materials and Methods*.

Glucuronidation of E_2 and E_1

UGT1A1, UGT1A3, UGT1A8, and UGT1A10 conjugate both E_2 and E_1, whereas UGT2B7 and UGT1A9 glucuronidate specifically E_2 and E_1, respectively (Table 3). Conjugation of E_2 was exclusively at position 3 for all UGTs tested, except for UGT2B7, which glucuronidated E_2 at position 17 and to a lesser extent by UGT1A3. K_m values for the formation of E_2-3G and E_2-17G were almost in the same range varying from 10 to 47 μM, whereas higher K_m values were observed for E_1-3G (38–90 μM). In general, lower velocity was observed for E_1-3G, compared with E_2-3G and E_2-17G conjugation, with the exception of UGT1A8, which demonstrated the highest V_{max} for both E_1-3G (142 pmol/min·mg) and E_2-3G (195 pmol/min·mg).

Depending on which UGT was involved, glucuronidation of E_1 and E_2 followed sigmoid and hyperbolic kinetic profiles (Fig. 2). Data for UGT1A1 and UGT1A3 best fitted a sigmoid profile for E_1 and E_2, and UGT1A9 and UGT2B7 exhibited hyperbolic profiles for the conjugation of E_1 and E_2. In turns, UGT1A8 and UGT1A10 demonstrated a kinetic profile dependent of the estrogenic substrate with a hyperbolic profile for E_2 and a sigmoid profile for E_1.

Catalytic efficiency values for the formation of E_2-3G and E_2-17G varied from 0.2 to 5.1 μl/min·mg, with UGT1A8 and UGT2B7 being the most efficient at glucuronidating E_2-3G and E_2-17G, respectively (Table 3). The highest value of catalytic efficiency was observed for E_1-3G with UGT1A8 (1.3 μl/min·mg).

Glucuronidation of 2-OHCE

Five UGTs, namely UGT1A1, UGT1A3, UGT1A8, UGT1A9, and UGT2B7, are responsible for the conjugation of 2-OHE_2 and 2-OHE_1 with the exception of UGT2B7, which shows activity for only 2-OHE_2. Although position 17 of 2-OHE_2 is not glucuronidated by UGTs (data not shown), every reactive UGT toward 2-OHCEs conjugates hydroxyls at both positions 2 and 3, except UGT1A1, which demonstrates a regioselective activity for the glucuronidation of

TABLE 2. Results of 16-h glucuronidation assays of a series of estrogens and metabolites by all known human UGT isoenzymes

UGTs	Estrogen glucuronides detected														
	E_1	E_2		2-OH				4-OH				2-MeO		4-MeO	
				E_1		E_2		E_1		E_2		E_1	E_2	E_1	E_2
	3G	3G	17G	2G	3G	2G	3G	3G	4G	3G	4G	3G	3G	3G	3G
1A1	(+)	++	−	−	++	−	++++	(+)	(+)	(+)	+	++	+++	(+)	++
1A3	+	(+)	(+)	(+)	+	−	++	(+)	(+)	(+)	−	++	++	(+)	(+)
1A4	−	−	−	−	−	−	−	−	−	−	−	−	−	−	−
1A5	−	−	−	−	−	−	−	−	−	−	−	−	−	−	−
1A6	−	−	−	−	−	−	−	−	−	−	−	−	−	−	−
1A7	−	−	−	−	−	−	−	−	−	−	−	−	−	−	−
1A8	++++	+++	−	++	+++	++	++	+++	++++	(+)	++	++++	+++	++++	++++
1A9	+	−	−	+	+++	(+)	++++	++	++++	−	+++	+++	++	++	++
1A10	(+)	++	−	−	−	−	−	−	−	−	(+)	++	++	(+)	(+)
2B4	−	−	−	−	+	−	−	−	−	−	(+)	+	+	−	−
2B7	−	−	(+)	−	(+)	−	++	−	++++	−	+++	−	−	−	−
2B10	−	−	−	−	−	−	−	−	−	−	−	−	−	−	−
2B11	−	−	−	−	−	−	−	−	−	−	−	−	−	−	−
2B15	−	−	−	−	−	−	−	−	−	−	−	−	−	−	−
2B17	−	−	−	−	−	−	−	−	−	−	−	−	(+)	−	−
2B28	−	−	−	−	−	−	−	−	−	−	−	−	−	−	−
LOQ	1	2	2	1	1	1	1	7.5	2	1	1	1	1	1	1

−, Negligible; (+), 101–500 ng/ml; +, 501–1,000 ng/ml; ++, 1,001–5,000 ng/ml; +++, 5,001–10,000 ng/ml; ++++, up to 10,000 ng/ml; LOQ, limit of quantification (ng/ml).

2-OHE_2 at position 2 and not for 2-OHE_1 at the same position (Table 3).

Glucuronidation of 2-OHCEs by UGT1A1, UGT1A3, and UGT1A8 display hyperbolic, sigmoid, or substrate inhibition profiles, whereas glucuronidation of 2-OHCEs by UGT1A9 and UGT2B7 follows a hyperbolic profile for both positions of 2-OHCEs (Fig. 3, A and B). The values of apparent K_m for conjugation at positions 2 or 3 of 2-OHE_2 vary widely, from 15 to 479 μM, whereas the K_m values are slightly higher for 2-OHE_1, especially at position 3, with UGT1A3 having a K_m of 587 μM (Table 3). In fact, the catalytic efficiencies of 2-OHE_2 conjugation by UGT1A8 and UGT2B7 are markedly higher than those of UGT1A1, UGT1A3, and UGT1A9. In fact, the catalytic efficiencies are as high as 11.3 μl/min·mg protein for glucuronidation at position 3-hydroxy of 2-OHE_2 by UGT2B7. Values are approximately 10-fold lower for conjugation at position 2-hydroxy, with the highest being at 1.3 μl/min·mg protein. On the other hand, the values of the catalytic efficiencies are similar for all enzymes in the conjugation of 2-OHE_1, with the exception of UGT1A1, which is much more efficient at conjugating 2-OHE_1 at position 3 (Table 3).

In summary, our data indicate that UGT2B7, UGT1A8, and UGT1A1 are the predominant conjugating enzymes of 2-OHE_2, whereas UGT1A1 is the major enzyme involved in 2-OHE_1-3G formation. It is important to note that all isoforms preferentially conjugate the 3-hydroxy of 2-OHCE.

Glucuronidation of 4-OHCE

As observed for $2\text{-OHE}_1/\text{E}_2$, $4\text{-OHE}_1/\text{E}_2$ can be conjugated in the two hydroxylated positions of ring A of the estrogen, whereas position 17 remains not conjugated (data not shown). For both 4-OHE_2 and 4-OHE_1, UGT1A1, UGT1A8, UGT1A9, and UGT2B7 have significant conjugating activities. In contrast to what was observed for 2-OHCEs, glucuronidation of 4-OHCEs by UGTs exhibits an hyperbolic profile, except for UGT1A1, which demonstrates substrate inhibition and sigmoid profiles for conjugation of both hydroxylated positions of 4-OHE_2 and 4-OHE_1, respectively (Fig. 3, C and D).

The K_m values for the 3 and 4 positions of 4-OHE_2 ranged from 38 to 118 μM, except UGT2B7, which has much higher affinity for 4-OHE_2 with K_m values of 10 and 22 μM at positions 4 and 3, respectively (Table 3). The catalytic efficiency of 4-OHE_1 glucuronidation at position 3 by the UGT isoforms appears relatively low, compared with conjugation of the same molecule at position 4. Two isoforms are major in the conjugation of position 4 of 4-OHE_2, namely UGT1A8 and UGT2B7, which demonstrate two of the highest V_{max} values observed, 4723 and 5235 pmol/min·mg, respectively. Although the conjugation of 4-OHE_1 was lower, compared with 4-OHE_2, UGT2B7 demonstrates the highest V_{max} at 8724 pmol/min·mg. The catalytic efficiency of UGT2B7 was about 5-fold higher for 4-OHE_2 (523.5 μl/min·mg protein), compared with 4-OHE_1 (140.7 μl/min·mg protein). Conjugation at the 3 hydroxyl position of 4-OHCE is preferentially catalyzed by UGT1A8, whereas the predominant substrate is 4-OHE_1. The relative V_{max} of 1975 pmol/min·mg and the catalytic efficiency of 10.7 μl/min·mg protein for UGT1A8 are at least 10-fold higher than the other UGTs catalyzing 4-OHE_2-3G and 4-OHE_1-3G. It is concluded that 4-OHE_1 is predominantly conjugated at position 4 by UGT2B7, whereas for 4-OHE_2, UGT1A8 and UGT2B7 are the predominant isoforms involved in the conjugation at position 4 (Table 3).

Glucuronidation of 2-MeOCE and 4-MeOCE

Our data demonstrate that five UGTs, namely UGT1A1, UGT1A3, UGT1A8, UGT1A9, and UGT1A10, conjugate 2-MeOCE. Of them, only UGT1A1 and UGT1A8 conjugate 4-MeOCE. As observed for other hydroxylated E, position 17

TABLE 3. Kinetic parameters for the glucuronidation of estrogens by most reactive human UGT isoenzymes

Substrates and UGTs	n	K_s	App. K_m (μM)	Rel. V_{max} (pmol/min/mg)	Catalytic efficiencies (μl/min/mg)	Kinetic profile	n	K_s	App. K_m (μM)	Rel. V_{max} (pmol/min/mg)	Catalytic efficiencies (μl/min/mg)	Kinetic profile
E_2				−3G						−17G		
UGT1A1	1.8		23	93	2.0	S			–	–	–	–
UGT1A3	1.8		47	39	0.4	S	1.9		35	13	0.2	S
UGT1A8			38	195	5.1	H			–	–	–	–
UGT1A10			17	3	0.2	H			–	–	–	–
UGT2B7			–	–	–	–			10	42	4.2	H
E_1				−3G								
UGT1A1	1.5		38	3	<0.1	S						
UGT1A3	1.9		77	50	0.3	S						
UGT1A8	1.9		55	142	1.3	S						
UGT1A9			54	4	0.1	H						
UGT1A10	1.6		90	3	<0.1	S						
2-OHE_2				−3G						−2G		
UGT1A1		17	165	1037	6.3	I	2.8		15	36	1.3	S
UGT1A3		6	479	1342	2.8	I	2.1		32	39	0.6	S
UGT1A8			20	188	9.4	H		10	102	126	1.2	I
UGT1A9			24	145	6.0	H			17	6	0.4	H
UGT2B7			33	372	11.3	H			33	14	0.4	H
2-OHE_1				−3G						−2G		
UGT1A1	1.4		19	326	9.4	S			–	–	–	–
UGT1A3			587	41	0.1	H	1.5		222	28	0.1	S
UGT1A8			40	88	2.2	H		72	52	38	0.7	I
UGT1A9			58	118	2.0	H			43	11	0.3	H
4-OHE_2				−3G						−4G		
UGT1A1		58	38	19	0.5	I		11	74	42	0.6	I
UGT1A8			118	119	1.0	H			105	4723	45.0	H
UGT1A9			55	17	0.3	H			53	1673	31.6	H
UGT2B7			22	48	2.2	H			10	5235	523.5	H
4-OHE_1				−3G						−4G		
UGT1A1	2.2		21	34	0.8	S	2.3		19	11	0.3	S
UGT1A8			184	1975	10.7	H			431	1538	3.6	H
UGT1A9			241	63	0.3	H			142	524	3.7	H
UGT2B7			–	–	–	–			62	8724	140.7	H
2-$MeOE_2$				−3G								
UGT1A1			49	222	4.5	H						
UGT1A3			49	154	3.1	H						
UGT1A8			66	1050	15.9	H						
UGT1A9			53	97	1.8	H						
UGT1A10			12	11	0.9	H						
2-$MeOE_1$				−3G								
UGT1A1			49	39	0.8	H						
UGT1A8			69	749	10.9	H						
UGT1A9			126	41	0.3	H						
4-$MeOE_2$				−3G								
UGT1A1			14	19	1.4	H						
UGT1A8			8	218	27.3	H						
4-$MeOE_1$				−3G								
UGT1A1			103	4	<0.1	H						
UGT1A8			111	275	2.5	H						

−, Not detected; n, Hill coefficient; K_s, inhibition constant; App. K_m, apparent K_m; Rel. V_{max}, relative V_{max}; H, hyperbolic profile; S, sigmoid profile; and I, substrate inhibition profile. Absolute glucuronidation activities were divided by the level of UGT protein and expressed as relative glucuronidation activities in picomoles per min per milligram.

was not conjugated. All UGTs displayed a hyperbolic kinetic profile (curves not shown).

Glucuronidation of 2- and 4-$MeOE_2$ occurs at higher rates than for 2- and 4-$MeOE_1$, these reactions being mostly catalyzed by UGT1A8. The K_m values of all substrates tested are almost in the same range, between 49 and 126 μM, with the exception for 2-$MeOE_2$ by UGT1A10, 4-$MeOE_2$ by UGT1A1, and UGT1A8 with K_m values of 12,

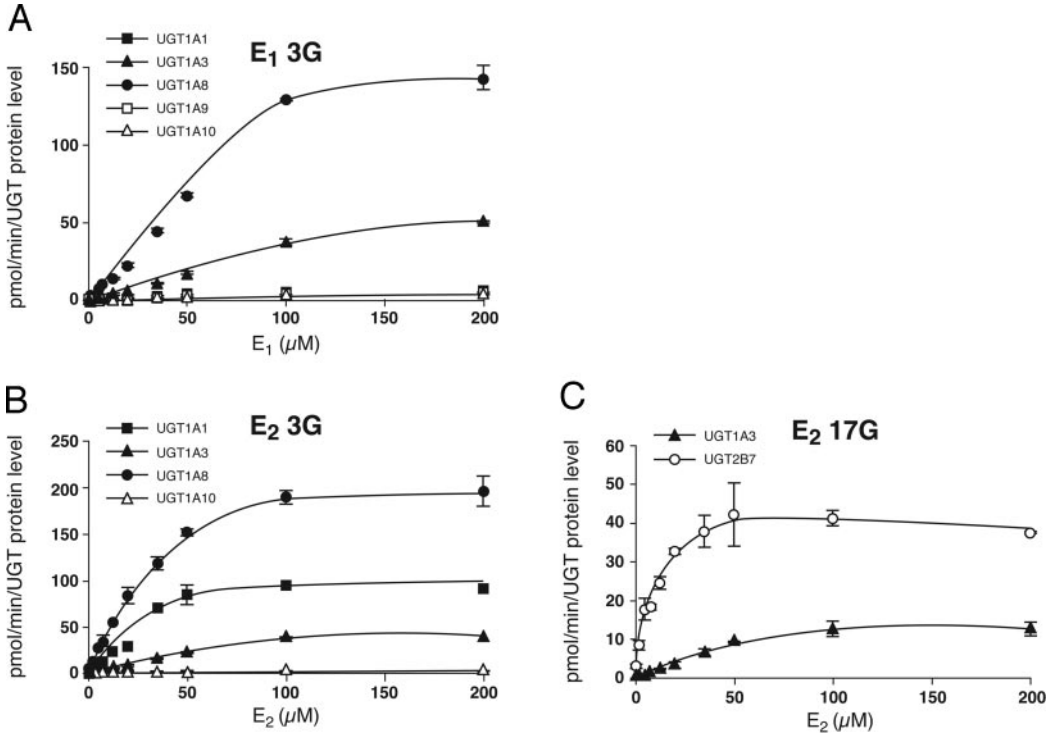

FIG. 2. Kinetic profiles for the glucuronidation of E_1 at position 3 (A) and E_2 at position 3 (B) and position 17 (C) by reactive human UGTs. Microsomal fractions from UGT-HEK293 cells and commercial microsomal fraction of UGT1A10 were incubated in the presence of varying estrogen concentrations from 0.5 to 200 μM for 1 h as described in *Materials and Methods*. Absolute glucuronidation activities were divided by the level of UGT protein assessed by Western blot and expressed as relative glucuronidation activities in picomoles per minute per milligram.

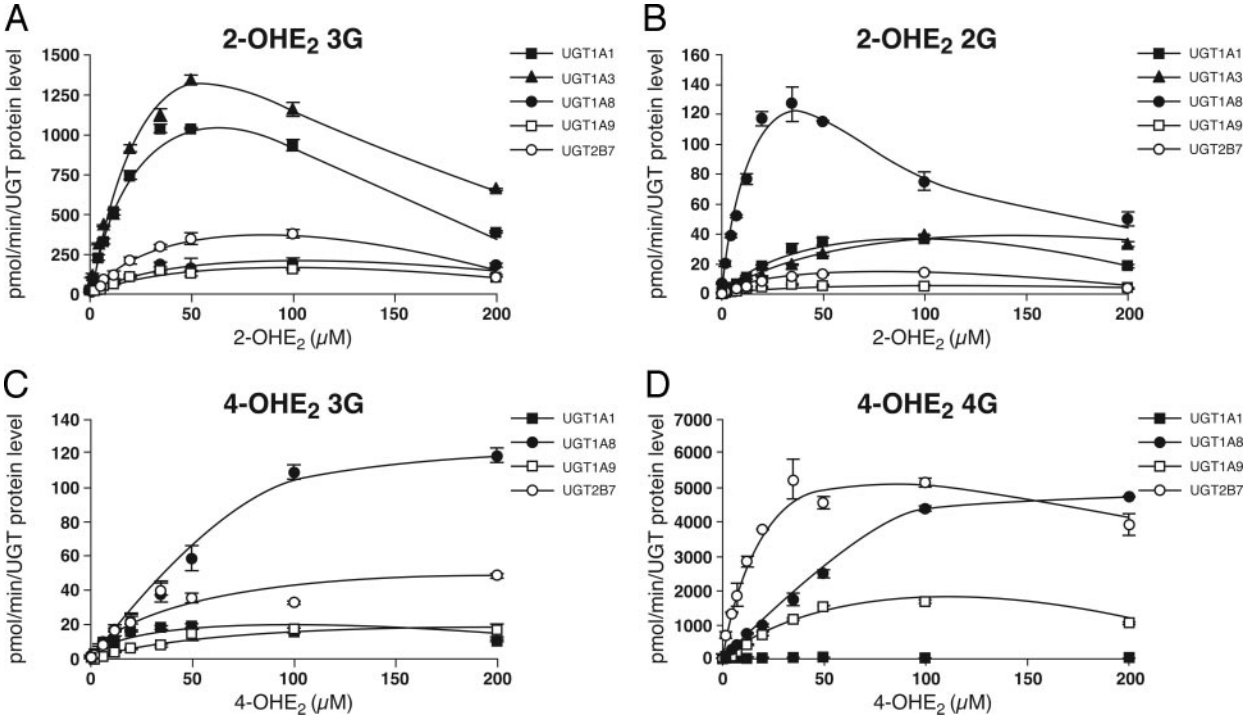

FIG. 3. Kinetic profiles for the glucuronidation of 2-OHE_2 (A, B) and 4-OHE_2 (C, D) by human UGTs. Microsomal fractions from UGT-HEK293 cells and commercial microsomal fraction of UGT1A10 were incubated in the presence of varying estrogen concentrations from 0.5 to 200 μM for 1 h as described in *Materials and Methods*. Absolute glucuronidation activities were divided by the level of UGT protein assessed by Western blot and expressed as relative glucuronidation activities in picomoles per minute per milligram.

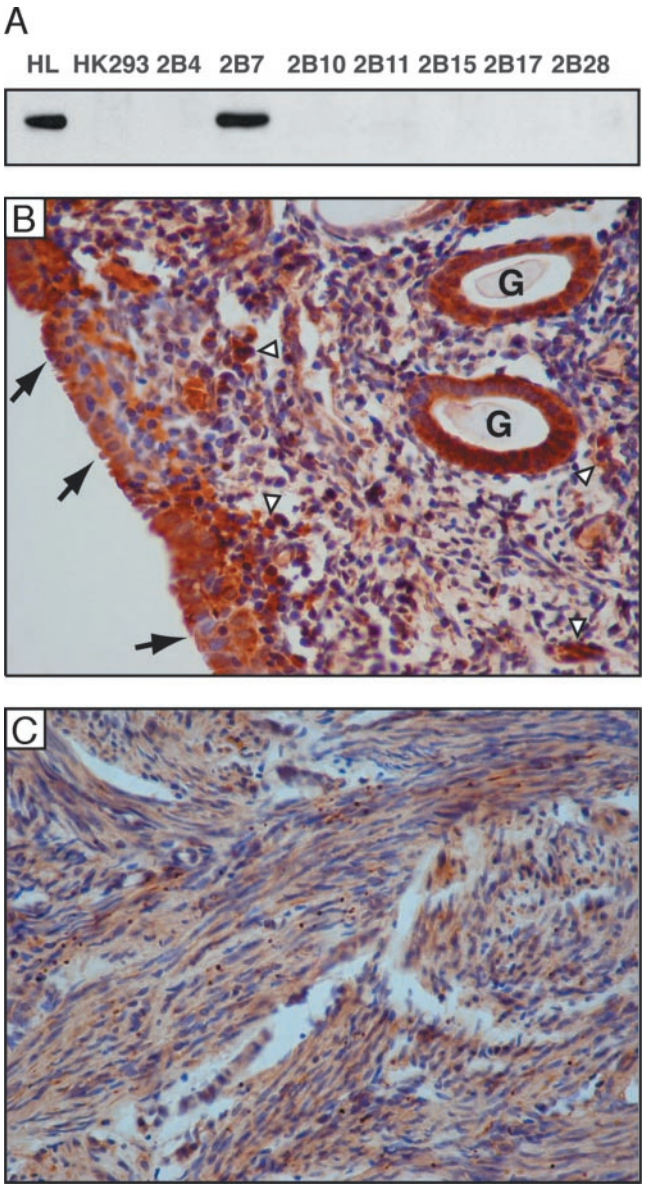

FIG. 4. A, Specificity of the polyclonal anti-UGT2B7 antibody assessed by Western blot analysis. Microsomal proteins (10 μg) of HK293 cells stably expressing UGT2B4, 2B7, 2B10, 2B11, 2B15, 2B17, and 2B28 were separated on a 10% SDS-PAGE. The anti-UGT2B7 antibody (dilution 1:2000) binds only to UGT2B7 proteins and human liver (HL) proteins (positive control) and not to HK293 cells (negative control). B and C, Immunohistochemistry performed on nonmalignant samples using human UGT2B7 antiserum as described in *Materials and Methods*. B, Endometrium. Immunolabeling is observed in the epithelial cells of uterine glands (G) and those lining the uterine cavity (*arrows*). Some stromal cells (*arrowheads*) are also labeled (×350). C, Myometrium. Immunostaining is present in smooth muscle cells (×350). No staining could be detected when the nonimmune serum was used (data not shown).

14, and 8 μM, respectively (Table 3). The catalytic efficiencies of 4-$MeOE_2$ and 2-$MeOE_2/E_1$ by UGT1A8 were the highest at 27.3, 15.9, and 10.9 μl/min·mg protein, respectively. UGT1A1 and UGT1A3 were also efficient at conjugating 2-$MeOE_2$ with catalytic efficiencies of 4.5 and 3.1 μl/min·mg protein, respectively.

Specificity of the polyclonal anti-UGT2B7 antibody

Western blot analysis using microsomal proteins (10 μg) of HK293 cells and HK293 cells stably expressing UGT2B4, 2B7, 2B10, 2B11, 2B15, 2B17, and 2B28 revealed that anti-UGT2B7 1809 antibody is specific to UGT2B7 protein. Microsomal proteins of human liver were used as positive control (Fig. 4A).

Expression of UGT2B7 in the uterus

The expression of the UGT2B7 was first assessed in endometrial tissues collected from six postmenopausal women by RT-PCR. Significant variation in UGT2B7 transcripts between endometrial samples was evident (Fig. 5). Immunostaining using specific antibodies to human UGT2B7 showed the presence of immunoreactive material in nonmalignant endometrium and myometrium. Both epithelial cells lining the glands and those covering the surface were strongly reactive (Fig. 4B). Endometrial stromal cells were also immunoreactive (Fig. 4B). In the myometrium, the vast majority of smooth muscle cells exhibited moderate immunolabeling (Fig. 4C). When the nonimmune serum was used, no staining could be detected (data not shown).

Discussion

In the present study, we thoroughly characterized the conjugation of E_2 and its main metabolites by all known human UGT enzymes. A newly developed HPLC/MS/MS method was used to accurately and specifically determine the products formed. The initial metabolic screening analyses show that a limited number of UGTs are capable of conjugating E_2; E_1; their hydroxylated metabolites, 2-OHCEs and 4-OHCEs; and their methoxyestrogen metabolites. Data indicate that the addition of the glucuronic acid is possible at positions 2, 3, and 4 of the catechol estrogens, whereas of all estrogens tested, only E_2 was conjugated at position 17 (Fig. 6). Detailed kinetic analyses point out that only six UGT enzymes of all 16 tested are involved in this process, namely UGT1A1, UGT1A3, UGT1A8, UGT1A9, UGT1A10, and UGT2B7, whereas a limited number of UGTs display regioselectivity for the estrogenic molecules. The data further indicate that UGT2B7, the most reactive UGT toward the genotoxic 4-OHCEs, is expressed at variable levels in endometrial tissue of postmenopausal women, even though the

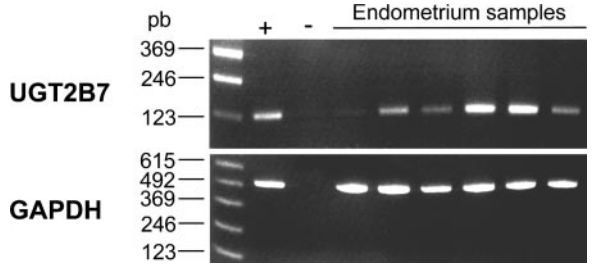

FIG. 5. Expression of human UGT2B7 relevant to 4-OHCEs glucuronidation in endometrium tissues as assessed by RT-PCR. Endometrium nonmalignant samples from six postmenopausal women were studied. The positive amplification (+) of GAPDH and 2B7 was performed in a human liver sample. The RT-PCR amplification products were analyzed by agarose gel electrophoresis and their identity further confirmed by direct sequencing of the RT-PCR products.

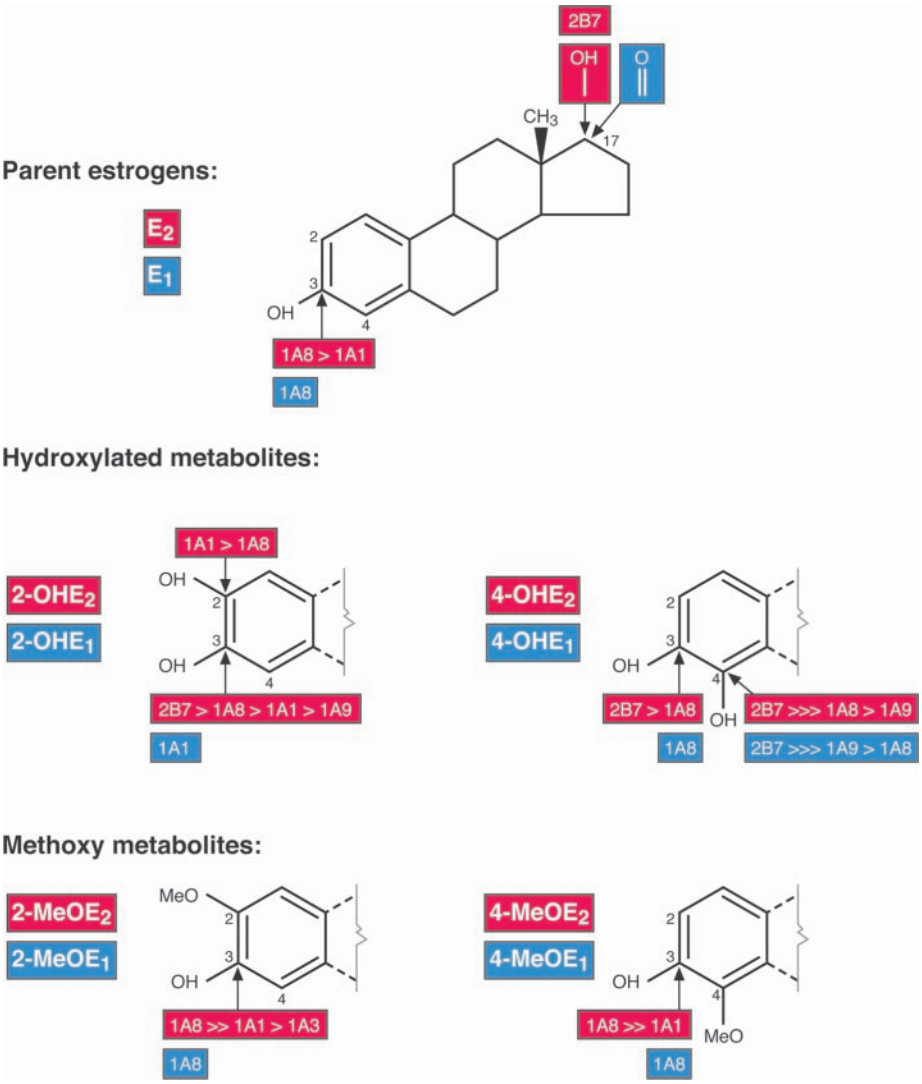

FIG. 6. Regioselectivity of human UGTs for parent estrogens, E_1 and E_2 as well as catechol estrogens, 2-OHE_1/E_2 and 4-OHE_1/E_2, and their methoxy metabolites, 2-$MeOE_1$/E_2 and 4-$MeOE_1$/E_2. The *red color* is used for E_2 and its metabolites, whereas the *blue color* refers to E_1 and its metabolites. Only UGTs with the highest catalytic efficiencies based on data presented in Table 3 are indicated.

sample size was limited. Our observations support the concept that E_1 and E_2 and their metabolites formed locally in estrogen sensitive tissues (5, 6) are conjugated by specific UGT enzymes *in situ* to achieve complete inactivation before their release in the circulation. The data further suggest a potential biological role of this metabolic pathway in the inactivation of genotoxic estrogens and that UGT2B7 is a key player in this process.

Compelling evidences that support glucuronidation as a major pathway of steroid inactivation and elimination in the liver and a number of steroid sensitive tissues have been published. For androgens, previous observations have clearly demonstrated the major role played by specific UGT2B isoenzymes, namely UGT2B7, UGT2B15, and UGT2B17, and their remarkable regioselectivity in the conjugation at positions 3 and/or 17 of dihydrotestosterone and its two major metabolites, and rostane-3α, 17β-diol, and androsterone (22). Although less attention was given to estrogen glucuronidation, few studies indicated that E_1 and E_2 may also be conjugated by specific UGTs in estrogen-sensitive tissues (15, 25, 33, 43, 44). Besides, E_1 and E_2 are converted into multiple hydroxylated metabolites in not only the liver but also several peripheral tissues (3). Recently Lee *et al.* (45) conducted a study aimed at characterizing the major metabolites of E_1 and E_2 by selected human CYPs. The authors concluded that the main oxidative pathway of E_1 and E_2 is likely by CYP1A1, CYP3A4, and CYP1B1, which predominantly leads to catechol estrogen production. In fact, CYP1A1 and CYP3A4 are responsible for the production of 2-OHCE and are expressed in estrogen-sensitive tissues, including the endometrium. CYP1B1 is exclusively found in extrahepatic tissues, namely the breast and endometrium, and produces 4-OHCE (5, 46, 47). These observations are concurrent with the recent findings of Rogan *et al.* (48), who demonstrated substantial amounts of CEs and their methoxyestrogen derivatives in breast tissue. However, in that study, the measurements of estrogen metabolites in the tissue were performed after treatment of the homogenate extracts with β-glucuronidase, thus indicating the potential for local formation of polar glucuronide derivatives. In fact, earlier studies demonstrated high concentrations of E_1 and E_2 glucuronides in the breast cyst fluid (23, 24), which is supported by the expression of several UGT isoenzymes (25, 33). The present findings suggest the formation of estrogen glucuronide derivatives in a second estrogen-sensitive tissue, namely the endometrium.

As demonstrated recently for CYPs (45), human UGTs catalyze the transfer of glucuronic acid to estrogenic substrates with a large range of catalytic efficiency and a unique stereoselectivity (Fig. 6). Even though more than one UGT is frequently involved in the conjugation of various estrogens, data indicate that several UGTs possess a distinctive regioselectivity for specific estrogenic molecules. The first general observation derived from our metabolic studies is that UGT1A family members conjugate estrogens at positions 2, 3, and 4 but not at position 17, with the exception of UGT1A3, which, however, shows a very low catalytic efficiency for this position. Previous observations have already indicated that UGT2B7 exclusively conjugates E_2 at position 17, whereas UGT1A1 was the enzyme responsible for the glucuronidation at position 3 (18, 28, 29). However, the present data clearly show that UGT1A8 is the predominant enzyme for conjugation of E_2 at position 3 followed by UGT1A1. The data further reveal that E_2 is the preferred estrogenic substrate for glucuronidation by human UGTs, compared with its keto metabolite E_1. This affirmation is also true for their corresponding 2-OHE_1/E_2, 4-OHE_1/E_2, and 4-$MeOE_1/E_2$ derivatives.

It is believed that the polarity of the estrogenic substrate has an important role in the subsequent conjugation via the glucuronidation pathway. Additional examination of data indicates that the glucuronidation of 2-OHE_2 and 2-OHE_1 is in large part at position 3 and that this conjugation is performed by UGT1A1, UGT1A8, and UGT2B7, whereas a modest activity is also observed for UGT1A3 and UGT1A9. In contrast, 4-OHE_2 and 4-OHE_1 are conjugated predominantly at position 4 and UGT2B7 is the major enzyme involved. In fact, it is the first time that the glucuronidation at position 4 of 4-OHE_2/E_1 is observed. Based on the *in vitro* enzyme kinetic data, the inactivation of 4-OHCEs is catalyzed by several enzymes but largely by UGT2B7. As previously observed for other estrogen metabolites, the change of the hydroxy group (E_2) to the keto group (E_1) at position 17 reduces by more than 50% the efficiency of UGT2B7. Recently Gestl *et al.* (25) have shown that the expression of UGT2B7 is particularly decreased in cancerous mammary gland tissue, compared with normal tissue. These authors suggested that UGT2B7 would protect the mammary gland from the genotoxic estrogen 4-OHE_1. Our data support the involvement of UGT2B7 in the inactivation of 4-OHCE and demonstrate its expression in a second estrogen-responsive tissue, the endometrium, which also expresses CYP1B1 involved in the local formation of 4-OHCE (5). In the uterus of postmenopausal women, we further showed using the UGT2B7 antibody immunoreactivity in the cells that also express CYP1B1, involved in the formation of 4-OHCEs. As for CYP1B1, UGT2B7 staining was predominantly seen in the cytoplasm in epithelial cells lining the uterine glands and those covering the surface in addition to smooth muscle cells of the myometrium (49, 50). These observations suggest that the formation of genotoxic 4-OHCE by CYP1B1 and subsequent conjugation by UGT2B7 may occur within the same cells of the uterus, supporting the protective role of UGT2B7.

The present study further highlights the previously unrecognized complexity of estrogen metabolism and suggests that the glucuronidation pathway may be significant in estrogen metabolism in extrahepatic tissue such as the mammary gland and uterus. Because E_2 and its 2-OH, 4-OH, and 2-MeO metabolites exert various biological effects, the present findings indicate that the glucuronidation pathway may represent a critical process in uterine cells, thus influencing estrogen exposure in this tissue. In agreement with this hypothesis, we recently demonstrated that a lower expression of UGT1A1, a UGT involved in the conjugation 2-OHCE and 2-MeOCE that mediate proliferative inhibitory effects (11–13), significantly decreases the risk of endometrial cancer (26). These data suggest that lower expression of UGT1A1 decreases the risk of endometrial cancer by reducing the excretion of the antiproliferative metabolite of E_2, 2-$MeOE_2$, in the endometrium. It is thus predicted from our kinetic data that additional UGTs, such as UGT2B7, play a significant role in protecting locally against 4-OHCEs by reducing their mutagenic potential in estrogen-responsive tissues such as the breast and uterus. In fact, the evaluation of the relative level of expression of the most reactive UGTs toward estrogens in nonmalignant endometrium tissues support the high level of expression of the UGT2B7 isoenzyme in this tissue (data not shown). Altogether, our data highlight the major importance of determining the presence of estrogen glucuronide derivatives in estrogen-sensitive tissues and into circulation.

Acknowledgments

We thank Sylvain Gauthier, Patrick Caron, Patrick Bélanger, Louise Désy, and Lyne Villeneuve for their expertise and technical assistance and Louis-Charles Fortier for preparation of illustrations. We thank Endorecherche for the glucuronide derivatives of 2-OHE_1/E_2, 4-OHE_1/E_2, 2-$MeOE_1/E_2$, and 4-$MeOE_1/E_2$. We also thank Dr. Jacques Lapointe for providing access to Sigma Plot/Enzyme Kinetics.

Received February 19, 2004. Accepted June 8, 2004.

Address all correspondence and requests for reprints to: Chantal Guillemette, Canada Research Chair in Pharmacogenomics, Pharmacogenomics Laboratory, Centre Hospitalier de l'Université Laval Research Center, T3-67, 2705 Boulevard Laurier, Québec G1V 4G2, Canada. E-mail: chantal.guillemette@crchul.ulaval.ca.

This work was supported by Canadian Institutes of Health Research (CIHR). C.G. is the chairholder of the Canadian Research Chair in Pharmacogenomics. J.L. is the recipient of a graduate studentship award from the CIHR. O.B. is the recipient of an undergraduate studentship award from the CIHR.

References

1. **Cauley JA, Lucas FL, Kuller LH, Stone K, Browner W, Cummings SR** 1999 Elevated serum estradiol and testosterone concentrations are associated with a high risk for breast cancer. Study of Osteoporotic Fractures Research Group. Ann Intern Med 130:270–277
2. **Persson I** 2000 Estrogens in the causation of breast, endometrial and ovarian cancers—evidence and hypotheses from epidemiological findings. J Steroid Biochem Mol Biol 74:357–364
3. **Jefcoate CR, Liehr JG, Santen RJ, Sutter TR, Yager JD, Yue W, Santner SJ, Tekmal R, Demers L, Pauley R, Naftolin F, Mor G, Berstein L** 2000 Tissue-specific synthesis and oxidative metabolism of estrogens. J Natl Cancer Inst Monogr 27:95–112
4. **Zhu BT, Conney AH** 1998 Functional role of estrogen metabolism in target cells: review and perspectives. Carcinogenesis 19:1–27
5. **Sasaki M, Kaneuchi M, Fujimoto S, Tanaka Y, Dahiya R** 2003 CYP1B1 gene in endometrial cancer. Mol Cell Endocrinol 202:171–176
6. **Sasaki M, Kaneuchi M, Sakuragi N, Dahiya R** 2003 Multiple promoters of catechol-*O*-methyltransferase gene are selectively inactivated by CpG hypermethylation in endometrial cancer. Cancer Res 63:3101–3106
7. **Liehr JG** 2000 Is estradiol a genotoxic mutagenic carcinogen? Endocr Rev 21:40–54
8. **Cavalieri EL, Li KM, Balu N, Saeed M, Devanesan P, Higginbotham S, Zhao J, Gross ML, Rogan EG** 2002 Catechol ortho-quinones: the electrophilic com-

pounds that form depurinating DNA adducts and could initiate cancer and other diseases. Carcinogenesis 23:1071–1077
9. **Cavalieri EL, Stack DE, Devanesan PD, Todorovic R, Dwivedy I, Higginbotham S, Johansson SL, Patil KD, Gross ML, Gooden JK, Ramanathan R, Cerny RL, Rogan EG** 1997 Molecular origin of cancer: catechol estrogen-3,4-quinones as endogenous tumor initiators. Proc Natl Acad Sci USA 94:10937–10942
10. **Cavalieri E, Frenkel K, Liehr JG, Rogan E, Roy D** 2000 Estrogens as endogenous genotoxic agents—DNA adducts and mutations. J Natl Cancer Inst Monogr 27:75–93
11. **Lakhani NJ, Sarkar MA, Venitz J, Figg WD** 2003 2-Methoxyestradiol, a promising anticancer agent. Pharmacotherapy 23:165–172
12. **D'Amato RJ, Lin CM, Flynn E, Folkman J, Hamel E** 1994 2-Methoxyestradiol, an endogenous mammalian metabolite, inhibits tubulin polymerization by interacting at the colchicine site. Proc Natl Acad Sci USA 91:3964–3968
13. **Fotsis T, Zhang Y, Pepper MS, Adlercreutz H, Montesano R, Nawroth PP, Schweigerer L** 1994 The endogenous oestrogen metabolite 2-methoxyoestradiol inhibits angiogenesis and suppresses tumour growth. Nature 368:237–239
14. **Suzuki T, Nakata T, Miki Y, Kaneko C, Moriya T, Ishida T, Akinaga S, Hirakawa H, Kimura M, Sasano H** 2003 Estrogen sulfotransferase and steroid sulfatase in human breast carcinoma. Cancer Res 63:2762–2770
15. **Albert C, Vallee M, Beaudry G, Belanger A, Hum DW** 1999 The monkey and human uridine diphosphate-glucuronosyltransferase UGT1A9, expressed in steroid target tissues, are estrogen-conjugating enzymes. Endocrinology 140: 3292–3302
16. **Longcope C, Gorbach S, Goldin B, Woods M, Dwyer J, Warram J** 1985 The metabolism of estradiol oral compared to intravenous administration. J Steroid Biochem 23:1065–1070
17. **Cheng Z, Rios GR, King CD, Coffman BL, Green MD, Mojarrabi B, Mackenzie PI, Tephly TR** 1998 Glucuronidation of catechol estrogens by expressed human UDP-glucuronosyltransferases (UGTs) 1A1, 1A3, and 2B7. Toxicol Sci 45:52–57
18. **Gall WE, Zawada G, Mojarrabi B, Tephly TR, Green MD, Coffman BL, Mackenzie PI, Radominska-Pandya A** 1999 Differential glucuronidation of bile acids, androgens and estrogens by human UGT1A3 and 2B7. J Steroid Biochem Mol Biol 70:101–108
19. **Raftogianis R, Creveling C, Weinshilboum R, Weisz J** 2000 Estrogen metabolism by conjugation. J Natl Cancer Inst Monogr 27:113–124
20. **Belanger A, Hum DW, Beaulieu M, Levesque E, Guillemette C, Tchernof A, Belanger G, Turgeon D, Dubois S** 1998 Characterization and regulation of UDP-glucuronosyltransferases in steroid target tissues. J Steroid Biochem Mol Biol 65:301–310
21. **Barbier O, Lapointe H, El Alfy M, Hum DW, Belanger A** 2000 Cellular localization of uridine diphosphoglucuronosyltransferase 2B enzymes in the human prostate by *in situ* hybridization and immunohistochemistry. J Clin Endocrinol Metab 85:4819–4826
22. **Belanger A, Pelletier G, Labrie F, Barbier O, Chouinard S** 2003 Inactivation of androgens by UDP-glucuronosyltransferase enzymes in humans. Trends Endocrinol Metab 14:473–479
23. **Belanger A, Caron S, Labrie F, Naldoni C, Dogliotti L, Angeli A** 1990 Levels of eighteen nonconjugated and conjugated steroids in human breast cyst fluid: relationships with cyst type. Eur J Cancer 26:277–281
24. **Belanger A, Labrie F, Angeli A** 1990 Unconjugated and glucuronide steroid levels in human breast cyst fluid. Ann NY Acad Sci 586:93–100
25. **Gestl SA, Green MD, Shearer DA, Frauenhoffer E, Tephly TR, Weisz J** 2002 Expression of UGT2B7, a UDP-glucuronosyltransferase implicated in the metabolism of 4-hydroxyestrone and all-trans retinoic acid, in normal human breast parenchyma and in invasive and *in situ* breast cancers. Am J Pathol 160:1467–1479
26. **Duguay Y, McGrath M, Lepine J, Gagne JF, Hankinson SE, Colditz GA, Hunter DJ, Plante M, Tetu B, Belanger A, Guillemette C, De Vivo I** 2004 The functional UGT1A1 promoter polymorphism decreases endometrial cancer risk. Cancer Res 64:1202–1207
27. **Cheng Z, Radominska-Pandya A, Tephly TR** 1998 Cloning and expression of human UDP-glucuronosyltransferase (UGT) 1A8. Arch Biochem Biophys 356: 301–305
28. **Senafi SB, Clarke DJ, Burchell B** 1994 Investigation of the substrate specificity of a cloned expressed human bilirubin UDP-glucuronosyltransferase: UDP-sugar specificity and involvement in steroid and xenobiotic glucuronidation. Biochem J 303:233–240
29. **Fisher MB, Vandenbranden M, Findlay K, Burchell B, Thummel KE, Hall SD, Wrighton SA** 2000 Tissue distribution and interindividual variation in human UDP-glucuronosyltransferase activity: relationship between UGT1A1 promoter genotype and variability in a liver bank. Pharmacogenetics 10: 727–739
30. **Mojarrabi B, Butler R, Mackenzie PI** 1996 cDNA cloning and characterization of the human UDP glucuronosyltransferase, UGT1A3. Biochem Biophys Res Commun 225:785–790
31. **Mackenzie PI, Owens IS, Burchell B, Bock KW, Bairoch A, Belanger A, Fournel-Gigleux S, Green M, Hum DW, Iyanagi T, Lancet D, Louisot P, Magdalou J, Chowdhury JR, Ritter JK, Schachter H, Tephly TR, Tipton KF, Nebert DW** 1997 The UDP glycosyltransferase gene superfamily: recommended nomenclature update based on evolutionary divergence. Pharmacogenetics 7:255–269
32. **Guillemette C** 2003 Pharmacogenomics of human UDP-glucuronosyltransferase enzymes. Pharmacogenomics J 3:136–158
33. **Guillemette C, Millikan RC, Newman B, Housman DE** 2000 Genetic polymorphisms in uridine diphospho-glucuronosyltransferase 1A1 and association with breast cancer among African Americans. Cancer Res 60:950–956
34. **Gagne JF, Montminy V, Belanger P, Journault K, Gaucher G, Guillemette C** 2002 Common human UGT1A polymorphisms and the altered metabolism of irinotecan active metabolite 7-ethyl-10-hydroxycamptothecin (SN-38). Mol Pharmacol 62:608–617
35. **Villeneuve L, Girard H, Fortier LC, Gagne JF, Guillemette C** 2003 Novel functional polymorphisms in the Ugt1A7 and Ugt1A9 glucuronidating enzymes in Caucasian and African-American subjects and their impact on the metabolism of Sn-38 and flavopiridol anticancer drugs. J Pharmacol Exp Ther 307:117–128
36. **Guillemette C, Levesque E, Beaulieu M, Turgeon D, Hum DW, Belanger A** 1997 Differential regulation of two uridine diphospho-glucuronosyltransferases, UGT2B15 and UGT2B17, in human prostate LNCaP cells. Endocrinology 138:2998–3005
37. **Barbier O, Belanger A** 2003 The cynomolgus monkey (*Macaca fascicularis*) is the best animal model for the study of steroid glucuronidation. J Steroid Biochem Mol Biol 85:235–245
38. **Pelletier G, Dupont E, Simard J, Luu-The V, Belanger A, Labrie F** 1992 Ontogeny and subcellular localization of 3β-hydroxysteroid dehydrogenase (3β-HSD) in the human and rat adrenal, ovary and testis. J Steroid Biochem Mol Biol 43:451–467
39. **Venkatakrishnan K, Von Moltke LL, Greenblatt DJ** 2001 Human drug metabolism and the cytochromes P450: application and relevance of *in vitro* models. J Clin Pharmacol 41:1149–1179
40. **Houston JB, Kenworthy KE** 2000 *In vitro-in vivo* scaling of CYP kinetic data not consistent with the classical Michaelis-Menten model. Drug Metab Dispos 28:246–254
41. **Court MH, Duan SX, Guillemette C, Journault K, Krishnaswamy S, Von Moltke LL, Greenblatt DJ** 2002 Stereoselective conjugation of oxazepam by human UDP-glucuronosyltransferases (UGTs): S-oxazepam is glucuronidated by UGT2B15, whereas R-oxazepam is glucuronidated by UGT2B7 and UGT1A9. Drug Metab Dispos 30:1257–1265
42. **Stone AN, Mackenzie PI, Galetin A, Houston JB, Miners JO** 2003 Isoform selectivity and kinetics of morphine 3- and 6-glucuronidation by human UDP-glucuronosyltransferases: evidence for atypical glucuronidation kinetics by UGT2B7. Drug Metab Dispos 31:1086–1089
43. **Guillemette C, De Vivo I, Hankinson SE, Haiman CA, Spiegelman D, Housman DE, Hunter DJ** 2001 Association of genetic polymorphisms in UGT1A1 with breast cancer and plasma hormone levels. Cancer Epidemiol Biomarkers Prev 10:711–714
44. **Guillemette C, Villeneuve L,** Substrate-dependent impact of a novel human UGT1A9 polymorphism. Proc 8th European ISSX Meeting, Dijon, France, 2003, p 27 (Abstract 117)
45. **Lee AJ, Cai MX, Thomas PE, Conney AH, Zhu BT** 2003 Characterization of the oxidative metabolites of 17β-estradiol and estrone formed by 15 selectively expressed human cytochrome p450 isoforms. Endocrinology 144:3382–3398
46. **Sarkar MA, Vadlamuri V, Ghosh S, Glover DD** 2003 Expression and cyclic variability of CYP3A4 and CYP3A7 isoforms in human endometrium and cervix during the menstrual cycle. Drug Metab Dispos 31:1–6
47. **Vadlamuri SV, Glover DD, Turner T, Sarkar MA** 1998 Regiospecific expression of cytochrome P4501A1 and 1B1 in human uterine tissue. Cancer Lett 122:143–150
48. **Rogan EG, Badawi AF, Devanesan PD, Meza JL, Edney JA, West WW, Higginbotham SM, Cavalieri EL** 2003 Relative imbalances in estrogen metabolism and conjugation in breast tissue of women with carcinoma: potential biomarkers of susceptibility to cancer. Carcinogenesis 24:697–702
49. **Bofinger DP, Feng L, Chi LH, Love J, Stephen FD, Sutter TR, Osteen KG, Costich TG, Batt RE, Koury ST, Olson JR** 2001 Effect of TCDD exposure on CYP1A1 and CYP1B1 expression in explant cultures of human endometrium. Toxicol Sci 62:299–314
50. **Muskhelishvili L, Thompson PA, Kusewitt DF, Wang C, Kadlubar FF** 2001 *In situ* hybridization and immunohistochemical analysis of cytochrome P450 1B1 expression in human normal tissues. J Histochem Cytochem 49:229–236

JCEM is published monthly by The Endocrine Society (http://www.endo-society.org), the foremost professional society serving the endocrine community.